Research Report
94 - 14

Space Vector PWM Control of Dual Three Phase Induction Machine Using Vector Space Decomposition

Y. Zhao and T.A. Lipo

Electrical & Computer Engineering
University of Wisconsin-Madison
Madison WI 53706-1691

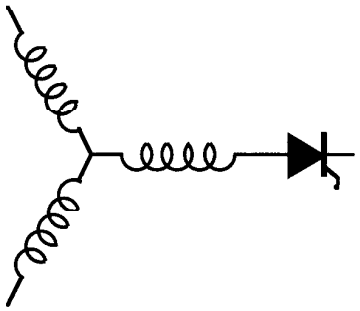

Wisconsin
Electric
Machines &
Power
Electronics
Consortium

University of Wisconsin-Madison
College of Engineering
Electrical & Computer Engineering Department
2559D Engineering Hall
1415 Johnson Drive
Madison WI 53706-1691

© June 1994 - Confidential

Space Vector PWM Control of Dual Three Phase Induction Machine Using Vector Space Decomposition

Y. Zhao T. A. Lipo
Department of Electrical and Computer Engineering
University of Wisconsin-Madison
1415 Johnson Drive
Madison, WI 53706

Abstract - **The technique of vector space decomposition control of voltage source inverter fed dual three phase induction machines is presented in this paper. By vector space decomposition, the analysis and control of the machine are accomplished in three two-dimensional orthogonal subspaces and the dynamics of the electromechanical energy conversion related and the non-electromechanical energy conversion related machine variables are thereby totally decoupled. A space vector PWM technique is also developed based on the vector space decomposition to limit the fifth, and seventh harmonic currents which in such a system would be otherwise difficult to control. The techniques developed in this paper can be generalized for the control of an induction machine with an arbitrary number of phases.**

I. INTRODUCTION

Dual three phase induction machine drive systems have long been considered a useful technique for enhancing power handling capabilities of drive systems under the limitations of semiconductor power device ratings. In such machines, two (or more) complete three phase windings are implemented in the same stator. In the most common such structure, two three phase windings are spatially phase shifted by 30 electrical degrees. In addition to using power devices with smaller individual ratings, it is also believed that drive systems with such multi-phase redundant structure will improve the reliability at the system level. However, when such systems are implemented with voltage source inverters and conventional six-step operation or space vector PWM control, surprisingly large and uncontrollable harmonic currents have been observed. Although this peculiarity has drawn attention from people working on this kind of system, the mechanism which causes the large harmonic content in the machine phase current still remains not well understood due to the complexity of the converter-machine model.

It is well known that the d-q-n reference frame has long been used successfully in the analysis and control of three phase electric machines. In this technology, the original three-dimensional vector space is decomposed into the direct sum of a d-q subspace and a zero sequence subspace, which is orthogonal to the d-q plane. By virtue of this decomposition, the components which produce rotating mmf and the components of zero sequence are totally decoupled, and thus the analysis and the control of the machine is simplified.

Since six currents flow, a dual three phase machine, or "six phase machine", is basically a six dimensional system. Therefore, the modeling and control problems of such systems must be addressed from the point of view of a six dimensional space. In this paper, the concept of decomposition is extended to the multi-phase case, a vector space decomposition control technique is developed. By vector space decomposition, the machine current and voltage vectors in the original six dimensional vector space are mapped into three two-dimensional orthogonal subspaces. As a result, the machine model can be described by three sets of decoupled equations. A new space vector PWM technique is also developed based on the vector space decomposition. The techniques presented in this paper can also be used to analyze the current source inverter fed dual three phase machines and generalized to control multi-phase induction machine drive systems.

II. VECTOR SPACE DECOMPOSITION AND TRANSFORMATION MATRIX

Consider the dual three phase, or 'six phase', induction machine drive system in Fig. 1 and the six phase voltage variables being sampled at any instant of time. The set of the sampled data voltage can be represented as a vector in a six dimensional space. As the variables are functions of time, the vector rotates about the origin and spans a surface in the six dimensional space. Geometrically, the control of the six phase machine is to position the vector on a certain surface in the six-dimensional vector space and rotate this vector at a desired speed. This makes the analysis and control of the six

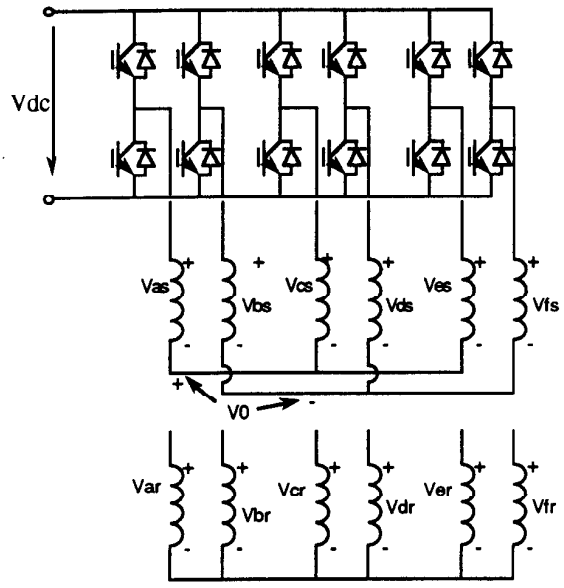

Fig. 1 Voltage Source Inverter Fed Dual Three Phase Induction Machine Drive System

phase machine a very difficult task. However, the analysis and control of the six phase machine can be greatly simplified. In the six phase machine, the voltages and currents can be characterized by defining the following vector:

$$S_k(\omega t)=[\cos k(\omega t)\quad \cos k(\omega t-\theta)\quad \cos k(\omega t-4\theta)\quad \cos k(\omega t-5\theta)\quad \cos k(\omega t-8\theta)\quad \cos k(\omega t-9\theta)] \quad (2.1)$$

where $\theta=30^0$, and k=0,1,3,5..., which denotes the order of harmonics. As the components of the vectors are functions of time, each vector spans a surface, or subspace, in the original six-dimensional space.

It can be proved that the subspaces corresponding to k=1,3,5 are orthogonal each other, i.e.

$$S_1 \bullet S_3^T = S_1 \bullet S_5^T = S_3 \bullet S_5^T = 0 \quad (0 \le \omega t \le 2\pi)$$

Therefore, the original six dimensional space can be expressed as the direct sum of these three orthogonal subspaces:

$$S = S_1 \oplus S_3 \oplus S_5$$

Furthermore, two orthogonal vectors can be chosen for each of the three subspaces as indicated below by selectively letting $\omega t = 0$ and $\pi/2$:

$k=1$

d: $[1 \quad \cos(\theta) \quad \cos(4\theta) \quad \cos(5\theta) \quad \cos(8\theta) \quad \cos(9\theta)]$

q: $[0 \quad \sin(\theta) \quad \sin(4\theta) \quad \sin(5\theta) \quad \sin(8\theta) \quad \sin(9\theta)]$

$k=5$

1: $[1 \quad \cos(5\theta) \quad \cos(8\theta) \quad \cos(\theta) \quad \cos(4\theta) \quad \cos(9\theta)]$

2: $[0 \quad \sin(5\theta) \quad \sin(8\theta) \quad \sin(\theta) \quad \sin(4\theta) \quad \sin(9\theta)]$

$k=3$

z_1: $[1 \quad 0 \quad 1 \quad 0 \quad 1 \quad 0]$

z_2: $[0 \quad 1 \quad 0 \quad 1 \quad 0 \quad 1]$

With the vectors used as the new basis of the six dimensional space, the following normalized coordinate transformation matrix results:

$$[T]=\frac{1}{\sqrt{3}}\begin{bmatrix} 1 & \cos(\theta) & \cos(4\theta) & \cos(5\theta) & \cos(8\theta) & \cos(9\theta) \\ 0 & \sin(\theta) & \sin(4\theta) & \sin(5\theta) & \sin(8\theta) & \sin(9\theta) \\ 1 & \cos(5\theta) & \cos(8\theta) & \cos(\theta) & \cos(4\theta) & \cos(9\theta) \\ 0 & \sin(5\theta) & \sin(8\theta) & \sin(\theta) & \sin(4\theta) & \sin(9\theta) \\ 1 & 0 & 1 & 0 & 1 & 0 \\ 0 & 1 & 0 & 1 & 0 & 1 \end{bmatrix} \quad (2.2)$$

and

$$[T]^{-1}=[T]^t=\frac{1}{\sqrt{3}}\begin{bmatrix} 1 & 0 & 1 & 0 & 1 & 0 \\ \cos(\theta) & \sin(\theta) & \cos(5\theta) & \sin(5\theta) & 0 & 1 \\ \cos(4\theta) & \sin(4\theta) & \cos(8\theta) & \sin(8\theta) & 1 & 0 \\ \cos(5\theta) & \sin(5\theta) & \cos(\theta) & \sin(\theta) & 0 & 1 \\ \cos(8\theta) & \sin(8\theta) & \cos(4\theta) & \sin(4\theta) & 1 & 0 \\ \cos(9\theta) & \sin(9\theta) & \cos(9\theta) & \sin(9\theta) & 0 & 1 \end{bmatrix} \quad (2.3)$$

The transformation possesses the following properties:

1. The fundamental component of the machine variables and the k^{th} order harmonics with $k = 12m \pm 5$, (m = 1,2,3,....) are transformed into the d-q subspace or 'd-q plane'.

It should be point out that the d-q axes have been chosen in the way such that they are coincide with the axes of air gap flux. Therefore, these variables will produce rotating mmf in the machine airgap and thus be electromechanical energy conversion related.

2. Harmonics with $k = 12m \pm 5$, ($m = 0,1,2,3,...$) are mapped into the 1-2 subspace; or '1-2 plane'. As the 1-2 subspace is orthogonal to the d-q subspace, it is expected that the variables on this plane will not generate any rotating mmf in the airgap and thus be non-electromechanical energy conversion related.

3. Zero sequence harmonics, which are also non-electromechanical energy conversion related, are mapped into the z1, z2 subspace.

III. MACHINE MODEL

The following assumptions have been made in deriving the six phase machine model:

1) machine windings are sinusoidally distributed;

2) flux path is linear.

Under these assumptions the voltage equations of the machine in the original six-dimensional space and the equations transformed to the orthogonal subspaces can be derived.

A. Machine Model in the Original Six-Dimensional Space

Stator voltage equation:

$$\begin{aligned}[V_s] &= [R_s]\cdot[i_s] + p\cdot([\lambda_s]) \\ &= [R_s]\cdot[i_s] + p\cdot([\lambda_{ss}]+[\lambda_{sr}]) \\ &= [R_s]\cdot[i_s] + p\cdot([L_{ss}]\cdot[i_s]+[L_{sr}]\cdot[i_r])\end{aligned} \quad (3.1)$$

Rotor voltage equation:

$$\begin{aligned}[V_r] &= [R_r]\cdot[i_r] + p\cdot([\lambda_r]) \\ &= [R_r]\cdot[i_r] + p\cdot([\lambda_{rr}]+[\lambda_{rs}]) \\ &= [R_r]\cdot[i_r] + p\cdot([L_{rr}]\cdot[i_r]+[L_{rs}]\cdot[i_s])\end{aligned} \quad (3.2)$$

where in these equations, according to the machine structure, the resistance and inductance matrices are defined as the follows.

$[R_s]$, $[R_r]$ - stator, rotor resistance matrices:

$$[R_s]=\begin{bmatrix} r_s & 0 & 0 & 0 & 0 & 0 \\ 0 & r_s & 0 & 0 & 0 & 0 \\ 0 & 0 & r_s & 0 & 0 & 0 \\ 0 & 0 & 0 & r_s & 0 & 0 \\ 0 & 0 & 0 & 0 & r_s & 0 \\ 0 & 0 & 0 & 0 & 0 & r_s \end{bmatrix}, \quad [R_r]=\begin{bmatrix} r_r & 0 & 0 & 0 & 0 & 0 \\ 0 & r_r & 0 & 0 & 0 & 0 \\ 0 & 0 & r_r & 0 & 0 & 0 \\ 0 & 0 & 0 & r_r & 0 & 0 \\ 0 & 0 & 0 & 0 & r_r & 0 \\ 0 & 0 & 0 & 0 & 0 & r_r \end{bmatrix}$$

$[L_{ss}]$ - stator self inductance matrix:

$$[L_{ss}] = L_{ls}\begin{bmatrix} 1 & 0 & 0 & 0 & 0 & 0 \\ 0 & 1 & 0 & 0 & 0 & 0 \\ 0 & 0 & 1 & 0 & 0 & 0 \\ 0 & 0 & 0 & 1 & 0 & 0 \\ 0 & 0 & 0 & 0 & 1 & 0 \\ 0 & 0 & 0 & 0 & 0 & 1 \end{bmatrix}$$

$$+L_{ms}\begin{bmatrix} 1 & \sqrt{3}/2 & -1/2 & -\sqrt{3}/2 & -1/2 & 0 \\ \sqrt{3}/2 & 1 & 0 & -1/2 & -\sqrt{3}/2 & -1/2 \\ -1/2 & 0 & 1 & \sqrt{3}/2 & -1/2 & -\sqrt{3}/2 \\ -\sqrt{3}/2 & -1/2 & \sqrt{3}/2 & 1 & 0 & -1/2 \\ -1/2 & -\sqrt{3}/2 & -1/2 & 0 & 1 & \sqrt{3}/2 \\ 0 & -1/2 & -\sqrt{3}/2 & -1/2 & \sqrt{3}/2 & 1 \end{bmatrix}$$

where

L_{ls}, L_{ms} - stator leakage and magnetizing inductance.

$[L_{rr}]$ - rotor self inductance matrix:

$$[L_{rr}] = L_{lr}\begin{bmatrix} 1 & 0 & 0 & 0 & 0 & 0 \\ 0 & 1 & 0 & 0 & 0 & 0 \\ 0 & 0 & 1 & 0 & 0 & 0 \\ 0 & 0 & 0 & 1 & 0 & 0 \\ 0 & 0 & 0 & 0 & 1 & 0 \\ 0 & 0 & 0 & 0 & 0 & 1 \end{bmatrix} +$$

$$\left(\frac{N_r}{N_s}\right)^2 L_{ms}\begin{bmatrix} 1 & \sqrt{3}/2 & -1/2 & -\sqrt{3}/2 & -1/2 & 0 \\ \sqrt{3}/2 & 1 & 0 & -1/2 & -\sqrt{3}/2 & -1/2 \\ -1/2 & 0 & 1 & \sqrt{3}/2 & -1/2 & -\sqrt{3}/2 \\ -\sqrt{3}/2 & -1/2 & \sqrt{3}/2 & 1 & 0 & -1/2 \\ -1/2 & -\sqrt{3}/2 & -1/2 & 0 & 1 & \sqrt{3}/2 \\ 0 & -1/2 & -\sqrt{3}/2 & -1/2 & \sqrt{3}/2 & 1 \end{bmatrix}$$

where

L_{lr} - rotor leakage inductance;

N_s, N_r - number of turns of stator and rotor winding.

$[L_{sr}]$ - stator-rotor mutual inductance matrix:

$$[L_{sr}] = \frac{N_r}{N_s} L_{ms} \bullet$$

$$\begin{bmatrix} c(\theta_r) & c(\frac{\pi}{6}-\theta_r) & c(\frac{4\pi}{6}-\theta_r) & c(\frac{5\pi}{6}-\theta_r) & c(\frac{8\pi}{6}-\theta_r) & c(\frac{9\pi}{6}-\theta_r) \\ c(\frac{11\pi}{6}-\theta_r) & c(\theta_r) & c(\frac{3\pi}{6}-\theta_r) & c(\frac{4\pi}{6}-\theta_r) & c(\frac{7\pi}{6}-\theta_r) & c(\frac{8\pi}{6}-\theta_r) \\ c(\frac{8\pi}{6}-\theta_r) & c(\frac{9\pi}{6}-\theta_r) & c(\theta_r) & c(\frac{\pi}{6}-\theta_r) & c(\frac{4\pi}{6}-\theta_r) & c(\frac{5\pi}{6}-\theta_r) \\ c(\frac{7\pi}{6}-\theta_r) & c(\frac{8\pi}{6}-\theta_r) & c(\frac{11\pi}{6}-\theta_r) & c(\theta_r) & c(\frac{3\pi}{6}-\theta_r) & c(\frac{4\pi}{6}-\theta_r) \\ c(\frac{4\pi}{6}-\theta_r) & c(\frac{5\pi}{6}-\theta_r) & c(\frac{8\pi}{6}-\theta_r) & c(\frac{9\pi}{6}-\theta_r) & c(\theta_r) & c(\frac{\pi}{6}-\theta_r) \\ c(\frac{3\pi}{6}-\theta_r) & c(\frac{4\pi}{6}-\theta_r) & c(\frac{7\pi}{6}-\theta_r) & c(\frac{8\pi}{6}-\theta_r) & c(\frac{11\pi}{6}-\theta_r) & c(\theta_r) \end{bmatrix}$$

where

c - the abbreviation of cos;

θ_r - rotor angular position.

$[L_{rs}]$ - rotor-stator mutual inductance matrix:

$$[L_{rs}] = \frac{N_r}{N_s} L_{ms} \bullet$$

$$\begin{bmatrix} c(\theta_r) & c(\frac{\pi}{6}+\theta_r) & c(\frac{4\pi}{6}+\theta_r) & c(\frac{5\pi}{6}+\theta_r) & c(\frac{8\pi}{6}+\theta_r) & c(\frac{9\pi}{6}+\theta_r) \\ c(\frac{11\pi}{6}+\theta_r) & c(\theta_r) & c(\frac{3\pi}{6}+\theta_r) & c(\frac{4\pi}{6}+\theta_r) & c(\frac{7\pi}{6}+\theta_r) & c(\frac{8\pi}{6}+\theta_r) \\ c(\frac{8\pi}{6}+\theta_r) & c(\frac{9\pi}{6}+\theta_r) & c(\theta_r) & c(\frac{\pi}{6}+\theta_r) & c(\frac{4\pi}{6}+\theta_r) & c(\frac{5\pi}{6}+\theta_r) \\ c(\frac{7\pi}{6}+\theta_r) & c(\frac{8\pi}{6}+\theta_r) & c(\frac{11\pi}{6}+\theta_r) & c(\theta_r) & c(\frac{3\pi}{6}+\theta_r) & c(\frac{4\pi}{6}+\theta_r) \\ c(\frac{4\pi}{6}+\theta_r) & c(\frac{5\pi}{6}+\theta_r) & c(\frac{8\pi}{6}+\theta_r) & c(\frac{9\pi}{6}+\theta_r) & c(\theta_r) & c(\frac{\pi}{6}+\theta_r) \\ c(\frac{3\pi}{6}+\theta_r) & c(\frac{4\pi}{6}+\theta_r) & c(\frac{7\pi}{6}+\theta_r) & c(\frac{8\pi}{6}+\theta_r) & c(\frac{11\pi}{6}+\theta_r) & c(\theta_r) \end{bmatrix}$$

B. Transformation of the voltage equations to the new reference frame

Applying the transformations (2.2) and (2.3) to the voltage equations (3.1) and (3.2) yields:

$$[T]\cdot[V_s] = [T]\cdot[R_s]\cdot[T]^{-1}\cdot[T]\cdot[i_s] + p\cdot\left([T]\cdot[L_{ss}]\cdot[T]^{-1}\cdot[T]\cdot[i_s] + [T]\cdot[L_{sr}]\cdot[T]^{-1}\cdot[T]\cdot[i_r]\right)$$

$$[T]\cdot[V_r] = [T]\cdot[R_r]\cdot[T]^{-1}\cdot[T]\cdot[i_r] + p\cdot\left([T]\cdot[L_{rr}]\cdot[T]^{-1}\cdot[T]\cdot[i_r] + [T]\cdot[L_{rs}]\cdot[T]^{-1}\cdot[T]\cdot[i_s]\right) \quad (3.3)$$

The dynamic models of the machine in the three subspaces can be derived from (3.3) and is illustrated by the following.

Machine model in d-q subspace:

$$\begin{bmatrix} v_{ds} \\ v_{qs} \end{bmatrix} = \begin{bmatrix} r_s & 0 \\ 0 & r_s \end{bmatrix}\cdot\begin{bmatrix} i_{ds} \\ i_{qs} \end{bmatrix} + \frac{d}{dt}\left\{\begin{bmatrix} L_{ls}+3L_{ms} & 0 \\ 0 & L_{ls}+3L_{ms} \end{bmatrix}\cdot\begin{bmatrix} i_{ds} \\ i_{qs} \end{bmatrix} + \frac{N_r}{N_s}L_{ms}\begin{bmatrix} 3\cos(\theta_r) & -3\sin(\theta_r) \\ 3\sin(\theta_r) & 3\cos(\theta_r) \end{bmatrix}\cdot\begin{bmatrix} i_{dr} \\ i_{qr} \end{bmatrix}\right\}$$

$$\begin{bmatrix} 0 \\ 0 \end{bmatrix} = \begin{bmatrix} r_r & 0 \\ 0 & r_r \end{bmatrix}\cdot\begin{bmatrix} i_{dr} \\ i_{qr} \end{bmatrix} + \frac{d}{dt}\left\{\begin{bmatrix} L_{lr}+3\left(\frac{N_r}{N_s}\right)^2 L_{ms} & 0 \\ 0 & L_{lr}+3\left(\frac{N_r}{N_s}\right)^2 L_{ms} \end{bmatrix}\cdot\begin{bmatrix} i_{dr} \\ i_{qr} \end{bmatrix} + \frac{N_r}{N_s}L_{ms}\begin{bmatrix} 3\cos(\theta_r) & 3\sin(\theta_r) \\ -3\sin(\theta_r) & 3\cos(\theta_r) \end{bmatrix}\cdot\begin{bmatrix} i_{ds} \\ i_{qs} \end{bmatrix}\right\} \quad (3.4)$$

Machine model in 1-2 subspace:

$$\frac{d}{dt}\begin{bmatrix} i_{1s} \\ i_{2s} \end{bmatrix} = \begin{bmatrix} -r_s/L_{ls} & 0 \\ 0 & -r_s/L_{ls} \end{bmatrix}\cdot\begin{bmatrix} i_{1s} \\ i_{2s} \end{bmatrix} + \begin{bmatrix} 1/L_{ls} & 0 \\ 0 & 1/L_{ls} \end{bmatrix}\begin{bmatrix} v_{1s} \\ v_{2s} \end{bmatrix} \quad (3.5)$$

Machine model in z1-z2 subspace:

$$\frac{d}{dt}\begin{bmatrix} i_{z1s} \\ i_{z2s} \end{bmatrix} = \begin{bmatrix} -r_s / L_{ls} & 0 \\ 0 & -r_s / L_{ls} \end{bmatrix} \cdot \begin{bmatrix} i_{z1s} \\ i_{z2s} \end{bmatrix} + \begin{bmatrix} 1/L_{ls} & 0 \\ 0 & 1/L_{ls} \end{bmatrix} \begin{bmatrix} v_{z1s} \\ v_{z2s} \end{bmatrix} \tag{3.6}$$

To write the machine model in the d-q subspace in state equation form, define:

$$\begin{bmatrix} \lambda_{ds} \\ \lambda_{qs} \\ \lambda_{dr} \\ \lambda_{qr} \end{bmatrix} = \begin{bmatrix} L_{ds,ds} & L_{ds,qs} & L_{ds,dr} & L_{ds,qr} \\ L_{qs,ds} & L_{qs,qs} & L_{qs,dr} & L_{qs,qr} \\ L_{dr,ds} & L_{dr,qs} & L_{dr,dr} & L_{dr,qr} \\ L_{qr,ds} & L_{qr,qs} & L_{qr,dr} & L_{qr,qr} \end{bmatrix} \cdot \begin{bmatrix} i_{ds} \\ i_{qs} \\ i_{dr} \\ i_{qr} \end{bmatrix} \tag{3.7}$$

where $\begin{bmatrix} L_{ds,ds} & L_{ds,qs} & L_{ds,dr} & L_{ds,qr} \\ L_{qs,ds} & L_{qs,qs} & L_{qs,dr} & L_{qs,qr} \\ L_{dr,ds} & L_{dr,qs} & L_{dr,dr} & L_{dr,qr} \\ L_{qr,ds} & L_{qr,qs} & L_{qr,dr} & L_{qr,qr} \end{bmatrix} =$

$$\begin{bmatrix} L_{ls}+3L_{ms} & 0 & 3\frac{N_r}{N_s}L_{ms}\cos(\theta_r) & -3\frac{N_r}{N_s}L_{ms}\sin(\theta_r) \\ 0 & L_{ls}+3L_{ms} & 3\frac{N_r}{N_s}L_{ms}\sin(\theta_r) & 3\frac{N_r}{N_s}L_{ms}\cos(\theta_r) \\ 3\frac{N_r}{N_s}L_{ms}\cos(\theta_r) & 3\frac{N_r}{N_s}L_{ms}\sin(\theta_r) & L_{lr}+3\left(\frac{N_r}{N_s}\right)^2 L_{ms} & 0 \\ -3\frac{N_r}{N_s}L_{ms}\sin(\theta_r) & 3\frac{N_r}{N_s}L_{ms}\cos(\theta_r) & 0 & L_{lr}+3\left(\frac{N_r}{N_s}\right)^2 L_{ms} \end{bmatrix}$$

variables. As a result, high switching frequency inverters are generally required in a voltage source inverter fed multi-phase induction machine drive. This is a drawback of such system.

IV. SPACE VECTOR PWM CONTROL STRATEGY

In the six phase machine drive system illustrated in Fig. 1, the stator windings can be connected either to a single neutral or to double neutrals, neutral wires are eliminated in both cases to reduce the dimension of the system.

The six phase voltage source inverter has totally 64 switching modes. By using the transformation matrix (2.2), the 64 voltage vectors corresponding to the switching modes are projected on the three planes. A space vector PWM control strategy which covers the control of the volt-seconds applied to the machine in all the three planes is then developed.

A. Transformation of the inverter output voltage vectors to the d-q, 1-2, and z1–z2 reference frame:

With the machine stator windings connected to the inverter without neutral wire, only line voltage of the machine corresponding to inverter switching modes are directly known. On the other hand, the transformation matrix (2.2) transforms the machine phase variables to the new d-q-1-2-z1-z2 reference frame. Therefore, it is necessary to develop

The d-q equation using flux as state variables can then be expressed as:

$$\frac{d}{dt}\begin{bmatrix} \lambda_{ds} \\ \lambda_{qs} \\ \lambda_{dr} \\ \lambda_{qr} \end{bmatrix} = \frac{-1}{D}\begin{bmatrix} r_s(L_{lr}+3\left(\frac{N_r}{N_s}\right)^2 L_{ms}) & 0 & -3r_s\frac{N_r}{N_s}L_{ms}\cos(\theta_r) & 3r_s\frac{N_r}{N_s}L_{ms}\sin(\theta_r) \\ 0 & r_s(L_{lr}+3\left(\frac{N_r}{N_s}\right)^2 L_{ms}) & -3r_s\frac{N_r}{N_s}L_{ms}\sin(\theta_r) & -3r_s\frac{N_r}{N_s}L_{ms}\cos(\theta_r) \\ -3r_r\frac{N_r}{N_s}L_{ms}\cos(\theta_r) & -3r_r\frac{N_r}{N_s}L_{ms}\sin(\theta_r) & r_r(L_{ls}+3L_{ms}) & 0 \\ 3r_r\frac{N_r}{N_s}L_{ms}\sin(\theta_r) & -3r_r\frac{N_r}{N_s}L_{ms}\cos(\theta_r) & 0 & r_r(L_{ls}+3L_{ms}) \end{bmatrix} \cdot \begin{bmatrix} \lambda_{ds} \\ \lambda_{qs} \\ \lambda_{dr} \\ \lambda_{qr} \end{bmatrix} + \begin{bmatrix} v_{as} \\ v_{qs} \\ 0 \\ 0 \end{bmatrix} \tag{3.8}$$

where $D = ac - b^2$

$$a = L_{ls}+3L_{ms}, \quad b = 3\frac{N_r}{N_s}L_{ms}, \quad c = L_{lr}+3\left(\frac{N_r}{N_s}\right)^2 L_{ms}$$

It is observed immediately from above equations that all the electromechanical energy conversion related variable components are mapped into the d-q subspace, or 'd-q-plane', and the non-electromechanical energy conversion related variable components are transformed to the 1-2 and z1-z2 planes. The dynamic equations of the machine are totally decoupled. As a result, the analysis and control of the machine can be greatly simplified.

It is also important to note that the non-electromechanical energy conversion related variables on the 1-2 and z1-z2 planes should be controlled to be as small as possible to reduce the extra losses in the machine. However, as can be seen from Eqs. (3.5) and (3.6), only stator resistance and leakage inductance are associated with these transformations from line voltages to phase voltages.

Fig. 2 shows two cases for the stator winding neutral point connection. In Fig. 2a, the stator windings are connected to a single neutral, the relation between the line and the phase voltages are defined by a full rank matrix as illustrated in Eq. (4.1).

$$\begin{bmatrix} v_{abs} \\ v_{bcs} \\ v_{cds} \\ v_{des} \\ v_{efs} \\ 0 \end{bmatrix} = \begin{bmatrix} 1 & -1 & 0 & 0 & 0 & 0 \\ 0 & 1 & -1 & 0 & 0 & 0 \\ 0 & 0 & 1 & -1 & 0 & 0 \\ 0 & 0 & 0 & 1 & -1 & 0 \\ 0 & 0 & 0 & 0 & 1 & -1 \\ 1 & 1 & 1 & 1 & 1 & 1 \end{bmatrix} \cdot \begin{bmatrix} v_{as} \\ v_{bs} \\ v_{cs} \\ v_{ds} \\ v_{es} \\ v_{fs} \end{bmatrix} \tag{4.1}$$

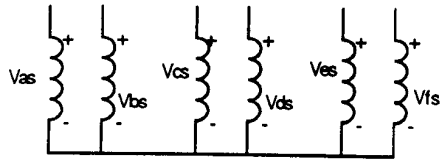

a)

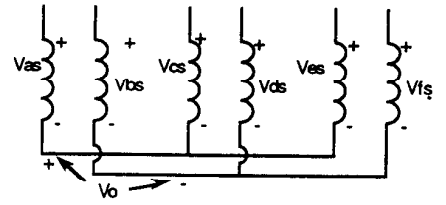

b)

Fig. 2 Stator Winding Connection
a) - Single Neutral Point Case
b) - Double Neutral Point Case

The transformation from line voltage to phase voltage can be derived from (4.1) by inverting the matrix. The resultant transformation is shown in (4.2).

$$\begin{bmatrix} v_{as} \\ v_{bs} \\ v_{cs} \\ v_{ds} \\ v_{es} \\ v_{fs} \end{bmatrix} = \frac{1}{6} \begin{bmatrix} 5 & 4 & 3 & 2 & 1 & 1 \\ -1 & 4 & 3 & 2 & 1 & 1 \\ -1 & -2 & 3 & 2 & 1 & 1 \\ -1 & -2 & -3 & 2 & 1 & 1 \\ -1 & -2 & -3 & -4 & 1 & 1 \\ -1 & -2 & -3 & -4 & -5 & 1 \end{bmatrix} \cdot \begin{bmatrix} v_{abs} \\ v_{bcs} \\ v_{cds} \\ v_{des} \\ v_{efs} \\ 0 \end{bmatrix} \quad (4.2)$$

Similarly, the transformation for the case of double neutral connection (Fig. 2 b)) can be derived and illustrated in Eq.'s (4.3), and (4.4).

Phase voltage to line voltage transformation:

$$\begin{bmatrix} v_{abs} \\ v_{bcs} \\ v_{cds} \\ v_{des} \\ v_{efs} \\ 0 \\ 0 \end{bmatrix} = \begin{bmatrix} 1 & 1 & -1 & 0 & 0 & 0 & 0 \\ -1 & 0 & 1 & -1 & 0 & 0 & 0 \\ 1 & 0 & 0 & 1 & -1 & 0 & 0 \\ -1 & 0 & 0 & 0 & 1 & -1 & 0 \\ 1 & 0 & 0 & 0 & 0 & 1 & -1 \\ 0 & 1 & 0 & 1 & 0 & 1 & 0 \\ 0 & 0 & 1 & 0 & 1 & 0 & 1 \end{bmatrix} \cdot \begin{bmatrix} v_0 \\ v_{as} \\ v_{bs} \\ v_{cs} \\ v_{ds} \\ v_{es} \\ v_{fs} \end{bmatrix} \quad (4.3)$$

Line voltage to phase voltage transformation:

$$\begin{bmatrix} v_0 \\ v_{as} \\ v_{bs} \\ v_{cs} \\ v_{ds} \\ v_{es} \\ v_{fs} \end{bmatrix} = \frac{1}{6} \begin{bmatrix} 2 & 0 & 2 & 0 & 2 & -2 & 2 \\ 4 & 4 & 2 & 2 & 0 & 2 & 0 \\ 0 & 4 & 4 & 2 & 2 & 0 & 2 \\ -2 & -2 & 2 & 2 & 0 & 2 & 0 \\ 0 & -2 & -2 & 2 & 2 & 0 & 2 \\ -2 & -2 & -4 & -4 & 0 & 2 & 0 \\ 0 & -2 & -2 & -4 & -4 & 0 & 2 \end{bmatrix} \cdot \begin{bmatrix} v_{abs} \\ v_{bcs} \\ v_{cds} \\ v_{des} \\ v_{efs} \\ 0 \\ 0 \end{bmatrix} \quad (4.4)$$

The next step is to combine the transformation (2.2) with the transformation (4.2), or (4.4) to transform the inverter voltage vectors corresponding to the 64 switching modes to the d-q-1-2-z1-z2 reference frame.

When the stator windings are connected to single neutral, the inverter voltage vectors are transformed to all the three planes as shown in Fig. 3 a) through Fig. 3 c). Note that all the voltage vectors on z1-z2 plane lie on a straight line. Therefore, the system is, in actuality, five dimensional.

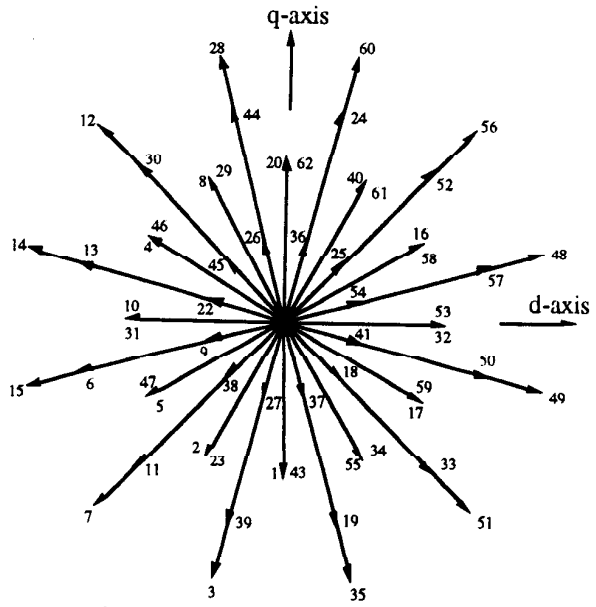

Switching Modes at Origin: 0,21,42,63
a)

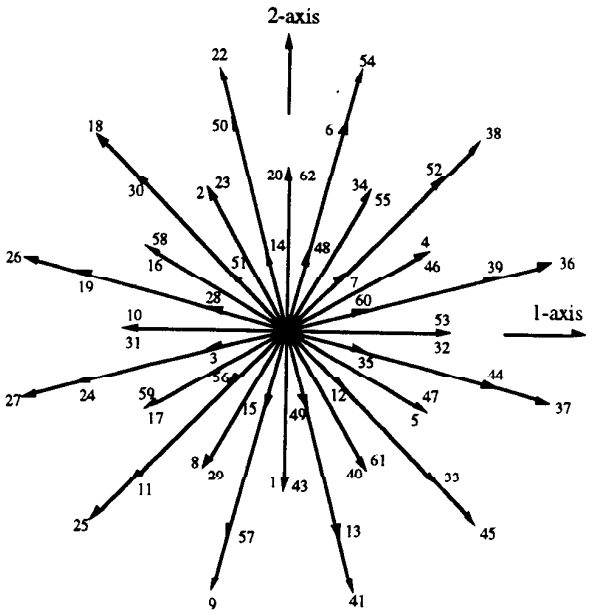

Switching Modes at Origin: 0,21,42,63
b)

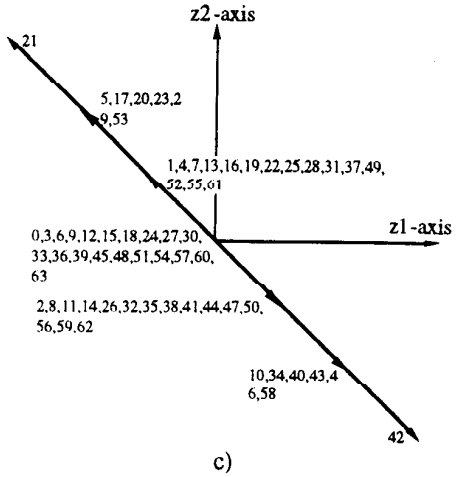

c)

Fig. 3 a) Inverter Voltage Vectors Projected on d-q Plane
b) Inverter Voltage Vectors Projected on 1-2 Plane
c) Inverter Voltage Vectors Projected on z1-z2 Plane

The decimal numbers in the figures denote the switching modes. When each decimal number is converted to a six digits binary number, the 1's in this number indicate that the upper switches in the corresponding switching arms are 'on', while the 0's indicate the 'on' state of the lower switches. The MSB of the number represents the switching state of phase *a*, the second MSB for phase *b* and so on.

In the case when the stator windings are connected to double neutrals as in Fig. 2 b), the projections of the inverter voltage vectors on the d-q, 1-2 planes remain the same as in the single neutral case. While on the z1-z2 plane, all the vectors are mapped to the origin. The resultant system is a four dimensional system, and the control of the six phase machine is further simplified.

B Space Vector PWM Control Strategy

The machine model has shown that only the voltages and currents in the d-q plane are related to electromechanical energy conversion. Therefore, the goal of the space vector PWM control is to synthesize the d-q voltage vectors to satisfy the machine control requirements, and, at the same time, to maintain the average volt-seconds on the 1-2 and z1-z2 planes to be zero during every sampling interval.

The space vector PWM strategy discussed in this paper is based on the double neutral topology as illustrated in Fig. 2. b). With stator windings connected to double neutrals the z1-z2 plane becomes trivial and the space vector PWM is performed only on the d-q, and 1-2 planes.

The space vector PWM strategy is accomplished by the following equation:

$$\begin{bmatrix} T_1 \\ T_2 \\ T_3 \\ T_4 \\ T_5 \end{bmatrix} = \begin{bmatrix} v_d^1 & v_d^2 & v_d^3 & v_d^4 & v_d^5 \\ v_q^1 & v_q^2 & v_q^3 & v_q^4 & v_q^5 \\ v_1^1 & v_1^2 & v_1^3 & v_1^4 & v_1^5 \\ v_2^1 & v_2^2 & v_2^3 & v_2^4 & v_2^5 \\ 1 & 1 & 1 & 1 & 1 \end{bmatrix} \cdot \begin{bmatrix} v_d^* T_s \\ v_q^* T_s \\ 0 \\ 0 \\ T_s \end{bmatrix} \qquad (4.5)$$

where v_x^k is the projection of the K^{th} voltage vector on the x-axis, and T_k the dwell time of that vector during time interval T_s. The v_d^* and v_q^* are the d-q plane reference voltages.

During each sampling period T_s, a set of five voltage vectors must be chosen to guarantee that T_k has a positive and unique solution. There are numerous ways of choosing such a set. The set used in this paper is illustrated in Fig. 4. In the method chosen, four adjacent voltage vectors are always chosen from the vectors which span the outermost polygon on the d-q plane according to the position of the reference voltage vector V_{dq}^*. For example, as indicated by the dots in Fig. 4 a), voltage vectors 49, 48, 56, and 60 are chosen when the reference voltage vector lies inside the triangle area between voltage vectors 48 and 56. In Fig. 4 b), the four voltage vectors spread out to cover the 1-2 plane, this makes it possible that the average volt-second on this plane be zero during every sampling interval.

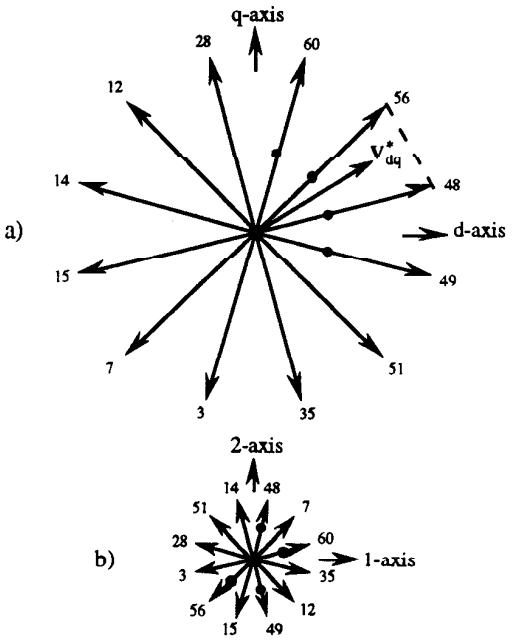

Fig. 4 Vectors Chosen by the Space Vector PWM

It is also noted from Fig. 4 b) that the vectors on the 1-2 plane have the smallest amplitude. Therefore, the proposed space vector PWM strategy will offer the maximum voltage output capability on the d-q plane yet keep the harmonics on the 1-2 plane a minimum.

C Simulation Results

The controller for the drive system using the developed vector space decomposition technique has been simulated and the results are shown in Fig. 5. For purpose of comparison, the control using the conventional space vector PWM technique and sine-triangle PWM have also been simulated and the results are shown in Fig. 6 and Fig. 7. In all the simulations, the inverter switching frequency was kept the same.

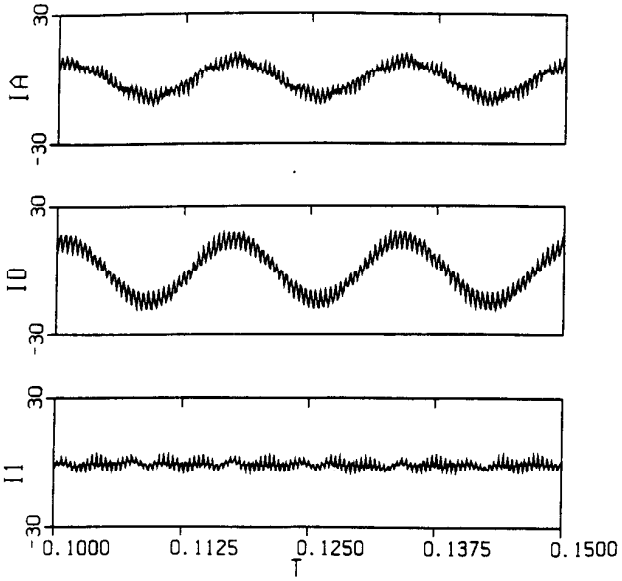

Fig. 5 Simulation Result Using Proposed Technique.
From top to bottom: machine phase current; current on d-q plane; current on 1-2 plane.

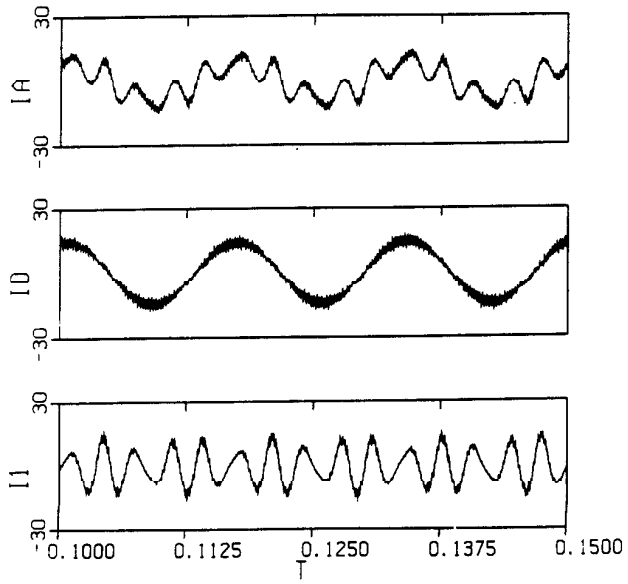

Fig. 6 Simulation Result Using Conventional Space Vector PWM Technique
From top to bottom: machine phase current; current on d-q plane; current on 1-2 plane.

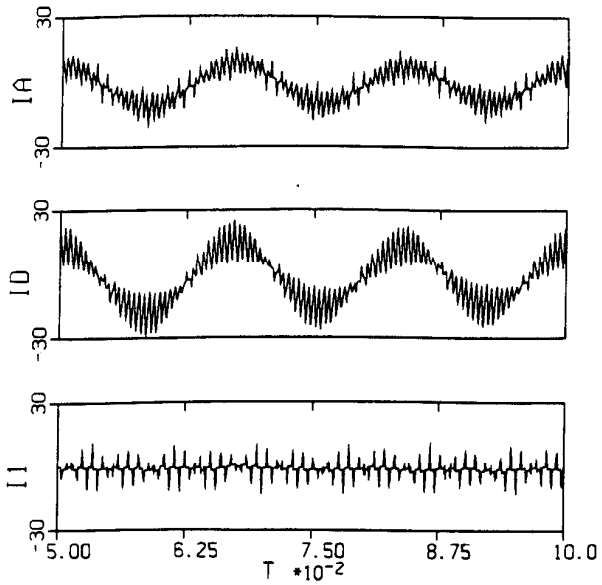

Fig. 7 Simulation Result Using Sine-Triangle PWM Technique
From top to bottom: machine phase current; current on d-q plane; current on 1-2 plane.

For the conventional space vector PWM, two adjacent voltage vectors plus one zero voltage vector at the origin are selected from the d-q plane. Since only the control over d-q plane variables is considered, the harmonic currents on the 1-2 plane are left free to flow. As a result, the amplitudes of these currents will be expected quite large. Fig. 6 shows the simulation results for this case, where considerable large fifth and seventh harmonic currents can be observed.

The simulation results in Fig. 7 suggests that the sine-triangle PWM technique is superior for the control of the six phase machine compared with the conventional space vector PWM. However, as being compared with the control technique proposed in this paper, the sine-triangle PWM technique produces larger amplitude of harmonic currents on the 1-2 plane because the voltage vectors generated by the sine and the triangular carrier wave crossing can not guarantee to have minimum projections on the 1-2 plane.

From the comparison of the simulation results, it is apparent that much better control performance can be achieved by using the proposed technique.

V. EXPERIMENTAL RESULTS

The dual three phase induction machine drive system examined in this paper has been built to test the proposed analysis and control technique. The implementation uses IGBT's for the power switching devices and a MOTOROLA DSP56000 microprocessor for the controller. A five horse power, four pole induction machine with thirty six stator slots was rewound to form a six pole, dual three phase machine for the purpose of the test. To compare the performance of the proposed space vector PWM with the conventional method, both strategies were implemented in software. Sampling frequencies of two kHz for the proposed technique and four kHz for the conventional approach have been chosen to maintain the switching frequency for an individual IGBT in

both cases to be equal at two kHz. Although this sampling frequency is far below the switching capability of the IGBT, however, is limited by the instruction execution speed and the minimum achievable timer interrupt interval of the DSP. For the same reason, the machine was operated for the tests at fifteen Hz rather than the rated sixty Hz.

The experimental results corresponding to the conventional space vector PWM are shown in Fig. 8. As having been expected, the harmonic currents on the 1-2 plane, i.e., the 5th, 7th, 17th, and 19th etc., are extraordinarily large due to the lack of control over currents on this plane. The performance of the proposed space vector PWM is illustrated in Fig. 9. Although the 5th and 7th harmonic currents are still appreciable due to the switching frequency limitation, very substantial reductions can be observed compared with the conventional method. The experimental results have sufficiently verified the correctness of the analysis and the feasibility of the proposed multi-phase induction machine control technique.

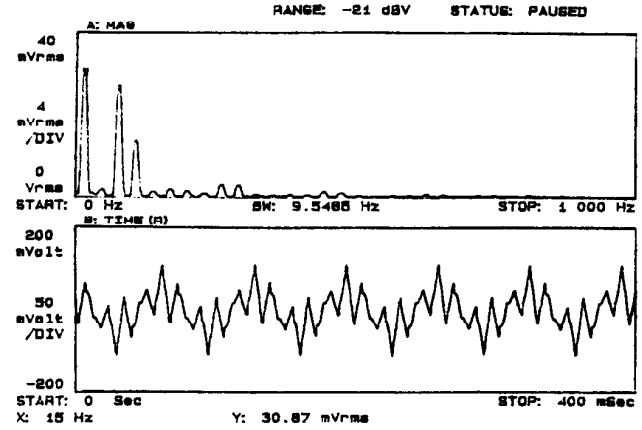

Fig. 8 Experimental Results Using the Conventional Space Vector PWM
Upper trace: current spectrum;
Lower trace: machine phase current, 5A(50mv)/div.

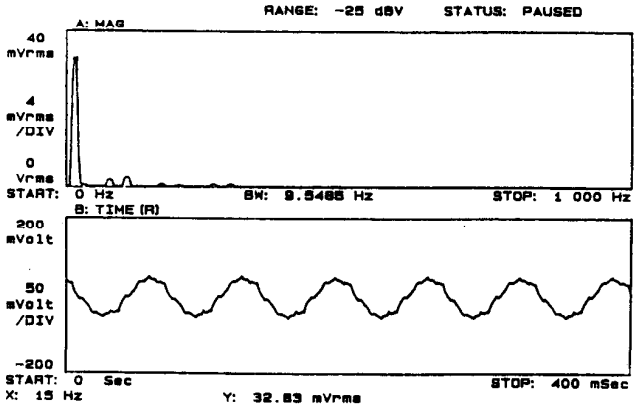

Fig. 9 Experimental Results Using the Proposed Space Vector PWM
Upper trace: current spectrum;
Lower trace: machine phase current, 5A(50mv)/div.

VI. CONCLUSIONS

This paper has presented a unified approach to space vector control of dual three phase induction machines. While the machine examined specifically deals with the dual three phase connection, it is clear that the approach may be readily extended to any machine having sinusiodally wound stator windings with any number of phases. It has often been stated that machines having a phase number greater than one are "all equivalent" from the modeling point of view. That is, it is said that all multiphase machines effectively reduce to the same d-q-0 equivalent circuit model. This paper has demonstrated that this perception is false. In particular, even when the phase currents sum to zero, m-3 zero sequence components exist. It is further shown that careful attention to control of these added zero sequence components are necessary to provide optimum current regulation of a multiphase machine.

VII. ACKNOWLEDGMENTS

The authors are indebted to the Electric Power Research Institute for funding of this research and to the member companies of WEMPEC for the facilities provided for the experimental test.

VIII. REFERENCES

[1] C. L. Fortescue, "Method of Symmetrical Co-ordinates Applied to the Solution of Polyphase Networks", AIEE Trans., Vol. 37, 1918, pp. 1027-1115.

[2] E.E. Ward, and H. Harer, "Preliminary Investigation of an Inverter Fed 5-Phase Induction Motor", IEEE Vol. 116, No. 6, June 1969, pp. 980-984.

[3] T.A. Lipo, "A d-q Model for Six Phase Induction Machines", International Conference on Electric Machines, September 15-17, 1980, Athens, Greece.

[4] M.A. Abbas, R. Christen, and T.M. Jahns, "Six-Phase Voltage Source Inverter Driven Induction Motor", IEEE Transactions on Industry Applications, Vol. 20, No. 5, September/October, 1984, pp. 1251-1259.

[5] R. J. Schilling, and H. Lee, "Engineering Analysis - A Vector Space Approach", John Wiley & Sons, Inc., New York, 1988.

[6] K. Gopakumar, V.T. Ranganathan, and S.R. Bhat, "Split-Phase Induction Motor Operation from PWM Voltage Source Inverter", IEEE Transactions on Industry Applications, Vol. 29, No. 5, September/October, 1993, pp. 927-932.